Stress triggering of the great Indian Ocean strike-slip earthquakes in a diffuse plate boundary zone

Kelly Wiseman[1] and Roland Bürgmann[1]

Received 19 September 2012; revised 18 October 2012; accepted 21 October 2012; published 28 November 2012.

[1] On April 11, 2012, two great magnitude 8+ earthquakes occurred within a two-hour period off the west coast of northern Sumatra, Indonesia, in the broadly distributed India-Australia plate boundary zone. The magnitude 8.6 mainshock holds the distinction of being both the largest instrumentally recorded strike-slip earthquake and the largest earthquake away from a recognized plate boundary fault. The mainshock involved sequential ruptures of multiple fault planes oriented nearly perpendicular to each other. The adjacent 2004 megathrust earthquake statically loaded the northern Wharton Basin oceanic lithosphere on both of the 2012 mainshock fault plane orientations, and greatly enhanced the rate of earthquake activity in the region for a year. Viscoelastic relaxation of the asthenosphere following the 2004 and 2005 megathrust earthquakes continued to positively stress the offshore region, correlating with the locations of later strike-slip earthquakes, including two magnitude 7+ and the 2012 magnitude 8+ earthquakes.
Citation: Wiseman, K., and R. Bürgmann (2012), Stress triggering of the great Indian Ocean strike-slip earthquakes in a diffuse plate boundary zone, *Geophys. Res. Lett.*, *39*, L22304, doi:10.1029/2012GL053954.

1. Introduction

[2] Plate tectonic theory assumes that the lithosphere is strong and rigid and that seismicity is mostly restricted to narrow plate boundaries. However, in the equatorial region of the Indian Ocean, the location of the M_w 8.6 and M_w 8.2 strike-slip earthquakes on April 11, 2012, the lithosphere is actively deforming in a broad zone between the rigid Indian and Australian plates (green shaded region in Figure 1). Seismic and geodetic data suggest that the deformation style changes from north-south shortening west of the Ninety East Ridge [*Deplus*, 2001; *Delescluse and Chamot-Rooke*, 2007] to north-south striking left-lateral shear in the Wharton Basin east of the Ninety East Ridge [*Deplus et al.*, 1998; *Deplus*, 2001; *Delescluse and Chamot-Rooke*, 2007] (Figure 1). Much of the diffuse boundary zone has an anomalously warm mantle, with temperatures above 800°C at 50 km depth (brown shaded regions in Figure 1) [*Shapiro et al.*, 2008]. In addition, the oceanic lithosphere is at its thinnest point along the entire Andaman-Sunda-Java trench system where it approaches northern Sumatra [*Shapiro et al.*, 2008]. The highest seismic strain-rates in the Indian Ocean are located in the northern Wharton Basin, where the thermally young, thin oceanic lithosphere is shearing along a network of NNE-SSW oriented fracture zones. These fractures are remnants from a fossil spreading ridge system and have accommodated at least 100 km of shear since the beginning of intraplate deformation eight million years ago [*Delescluse and Chamot-Rooke*, 2007]. A deep seismic reflection profile ~100 km north of the mainshock epicenter has imaged shallow offset sediments near these NNE-SSW structures, indicating that these fractures are still actively shearing [*Singh et al.*, 2011]. *Sager et al.* [2010] has observed roughly E-W oriented canyons and troughs along the northern Ninety East Ridge using gravity gradient data, indicative of past spreading accommodated by normal faulting. Seismic profiles along the Ninety East Ridge demonstrate that the faults were active when the ridge formed, and some of the faults penetrate the entire sediment column, evidence of active faulting.

2. Seismicity in the Northern Wharton Basin

[3] The style of seismicity in the northern Wharton Basin, between the Ninety East Ridge and the Sunda Trench, is dominated by strike-slip mechanisms, which accommodate the ongoing left-lateral shear in the diffuse plate boundary zone. The yellow "beach balls" in Figure 1 (http://www.globalcmt.org) depict the focal mechanisms for all of the strike-slip earthquakes in the incoming Indian and Australian plates, west of the Andaman-Sunda-Java Trench, from the start of the Global CMT catalog in 1976 until the April 2012 earthquakes. The mechanisms are very similar to the focal mechanisms for the two April, 2012 earthquakes (shown in red), and are consistent with either left-lateral strike-slip motion on the NNE-SSW oriented fractures, or right-lateral motion on WNW-ESE oriented planes.

[4] The 2004 M_w 9.2 Sumatra-Andaman megathrust earthquake [*Shearer and Bürgmann*, 2010] was the largest tectonic event in Southeast Asia over the last several hundred years and it fundamentally changed the stress state and seismicity rates in the surrounding lithosphere [*Wiseman and Bürgmann*, 2011]. The megathrust plate-interface has been especially active south of the 2004 rupture, including a M_w 8.7 earthquake in 2005 that was likely stress triggered by the nearby 2004 earthquake [*McCloskey et al.*, 2005; *Nalbant et al.*, 2005] and a M_w 8.4 earthquake in 2007. There has also been enhanced seismicity throughout the rest of the subduction zone: in the overriding Sunda Plate [*Wiseman et al.*, 2011], in the Andaman back-arc region [*Cattin et al.*, 2009; *Sevilgen et al.*, 2012], in the downgoing slab – including the 2009 M_w 7.6 Padang earthquake [*McCloskey et al.*, 2010; *Wiseman et al.*, 2012], and in the incoming Indian and Australian plates (Figure 2).

[1]Berkeley Seismological Laboratory, University of California, Berkeley, California, USA.

Corresponding author: K. Wiseman, Berkeley Seismological Laboratory, University of California, 307 McCone Hall, Berkeley, CA 94720, USA. (kelly@seismo.berkeley.edu)

0094-8276/12/2012GL053954

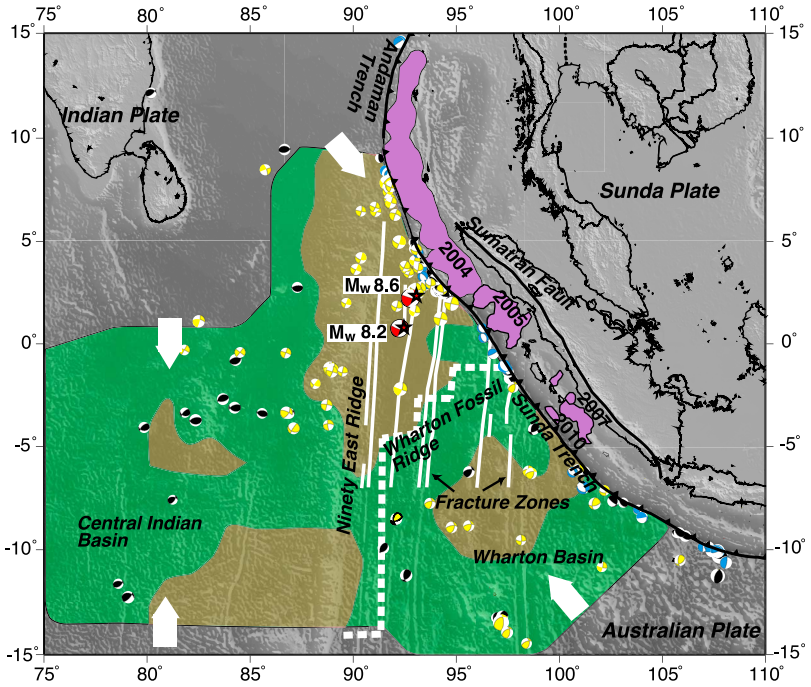

Figure 1. Tectonic overview of the India-Australia Plate. The diffuse boundary between the Indian and Australian plates is shaded green [*Delescluse and Chamot-Rooke*, 2007] and overlays the bathymetry [*Amante and Eakins*, 2009]. The overlapping regions with anomalously high lithospheric temperatures are shaded brown [*Shapiro et al.*, 2008]. Fractures and ridges within Wharton Basin are from *Singh et al.* [2011] and *Shapiro et al.* [2008]. All of the focal mechanisms for earthquakes in the India-Australia plate west of the Andaman-Sunda-Java Trench from 1976 until the 2012 mainshock (Global CMT catalog) are shown; strike-slip events are colored yellow, reverse events are colored black, and normal events are colored blue. The white arrows illustrate the orientations of maximum compression in the Central Indian Basin and Wharton Basin. Rupture patches for recent megathrust earthquakes are colored purple [*Chlieh et al.*, 2007; *Konca et al.*, 2007, 2008; *Hill et al.*, 2012].

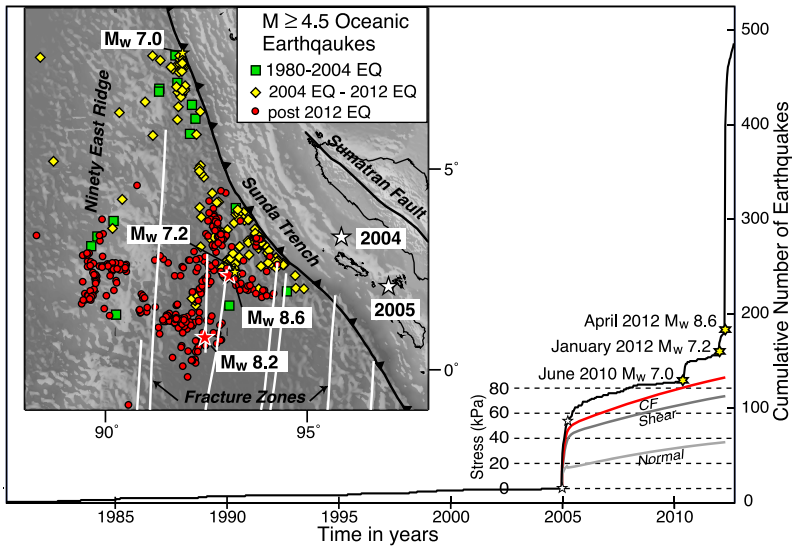

Figure 2. Northern Wharton Basin seismicity. The cumulative number of M ≥ 4.5 earthquakes (ISC and NEIC catalogs) in the Northern Wharton Basin, west of the Sunda Trench, from 1980 until September 10, 2012 is plotted in black. The yellow stars mark large earthquakes within the catalog region that initiated seismicity rate increases, and the 2004 and 2005 megathrust earthquakes (not in the region) are marked with white stars. The epicentral locations of the events are shown in the map inset. The cumulative coseismic and postseismic stress changes from the 2004 and 2005 earthquakes [*Chlieh et al.*, 2007; *Konca et al.*, 2007], resolved on the initial WNW-ESE fault plane orientation at the 2012 hypocenter are plotted in red and gray (see Figure S9 in the auxiliary material for longer stress time series).

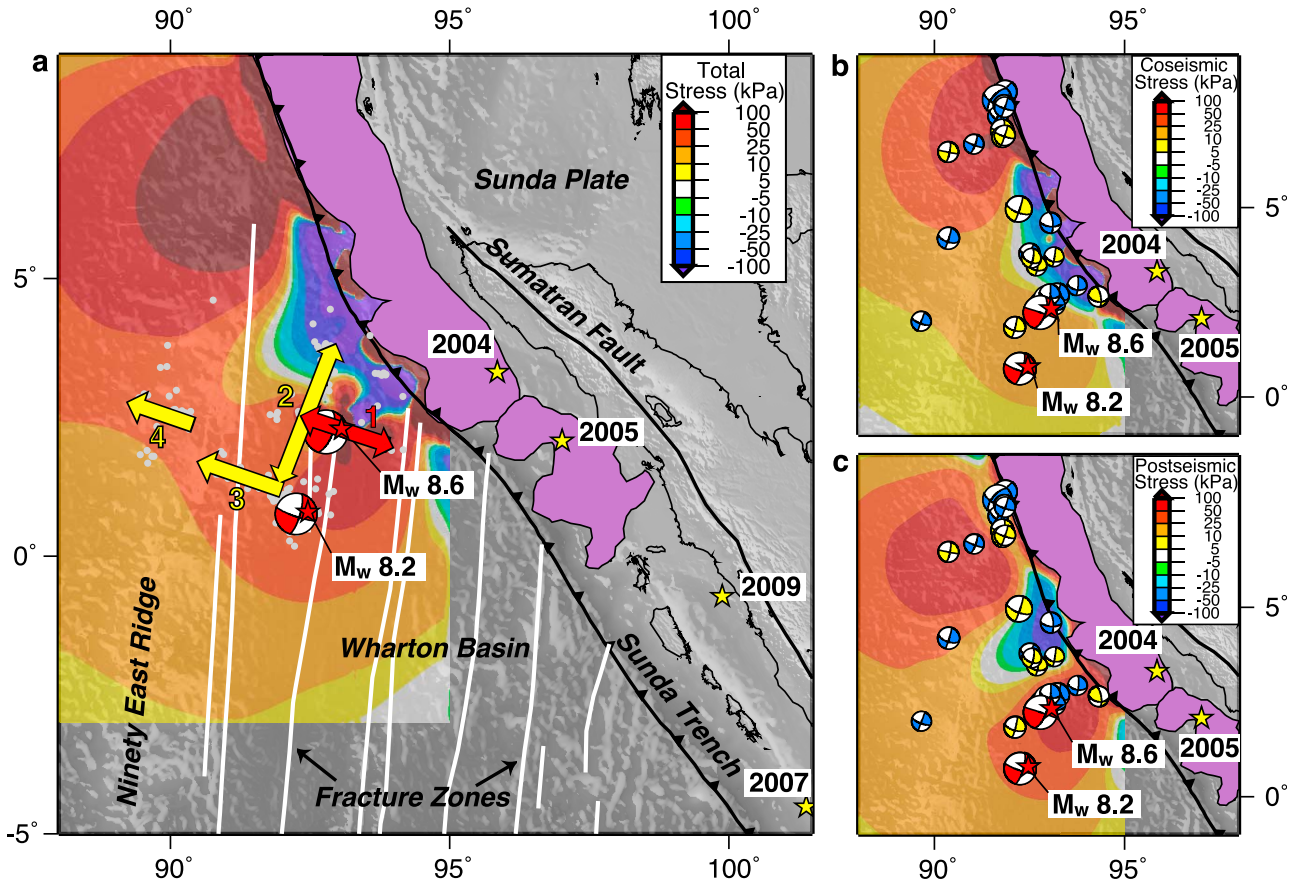

Figure 3. Recent stress changes in the Indian Ocean. (a) Total stresses induced by the 2004 [*Chlieh et al.*, 2007], 2005 [*Konca et al.*, 2007], and January M7.2 (http://earthquake.usgs.gov/earthquakes/eqinthenews/2012/usc0007ir5/finite_fault.php) earthquakes, resolved at the 20 km hypocentral depth of the mainshock on the orientation of the initial WNW-ESE (red) fault plane [*Meng et al.*, 2012]. Gray circles mark the first 12 days of the aftershock sequence (NEIC catalog). (b) Coseismic stresses induced by the 2004 and 2005 earthquakes. The yellow focal mechanisms highlight the strike-slip earthquakes during the first year following the 2004 earthquake and the blue focal mechanisms depict the remaining strike-slip events before the 2012 mainshock (Global CMT catalog). (c) Cumulative postseismic stresses induced by the 2004 and 2005 earthquakes at the time of the 2012 earthquake.

[5] The seismicity rate in the northern Wharton Basin increased dramatically following the 2004 earthquake. Figure 2 shows the cumulative number of M ≥ 4.5 earthquakes, the magnitude of completeness for the time period 1980–2012 (ISC and NEIC catalogs). The increased seismicity rate following the 2004 earthquake decays back to the background level within a year, but spikes again in 2010 and early 2012 following M 7+ strike-slip earthquakes.

3. The April 11, 2012 Ruptures

[6] The 2012 mainshock initiated at 20 km depth and the aftershock pattern (gray circles in Figure 3a, NEIC catalog), along with several back-projection rupture propagation models [*Meng et al.*, 2012; *Satriano et al.*, 2012; *Yue et al.*, 2012], suggests complex rupture on multiple fault planes. It appears that the mainshock started with bilateral propagation away from the hypocenter on an WNW-ESE oriented plane (red fault segment in Figure 3a) and then bilaterally ruptured a NNE-SSW oriented plane to the west of the hypocenter (yellow segment labeled 2). It ended with slip on two additional WNW-ESE oriented segments to the south, near the eventual M_w 8.2 aftershock (yellow segments labeled 3 and 4) [*Meng et al.*, 2012]. The second rupture segment is consistent with left-lateral faulting on one of the roughly N-S oriented fractures within the Wharton Basin. The fourth rupture segment appears to have reactivated one of the roughly E-W oriented faults along the Ninety East Ridge [*Sager et al.*, 2010], and the first and third fault segments suggest similar structural features extend into the Wharton Basin.

[7] *Yue et al.* [2012] resolved the spatial distribution of slip on the multiple fault segments using finite fault inversions, with geometry constrained by back-projections of short- and long-period seismic energy. They found that the largest moment release was on the initial WNW-ESE segment, with a peak slip of ~37 m [*Yue et al.*, 2012]. The first three segments also contained between ~5–20 m of deep slip, below the hypocenter, extending to ~50 km depth. This helps to explain the 40 km centroid depth (Global CMT and USGS CMT), the best point source location for the rupture, which was 20 km deeper than the hypocenter – where the earthquake initiated. *McGuire and Beroza* [2012] argue that the deeper slip would require a failure mode other than typical frictional failure, and suggest highly localized zones of viscous failure in the upper oceanic mantle.

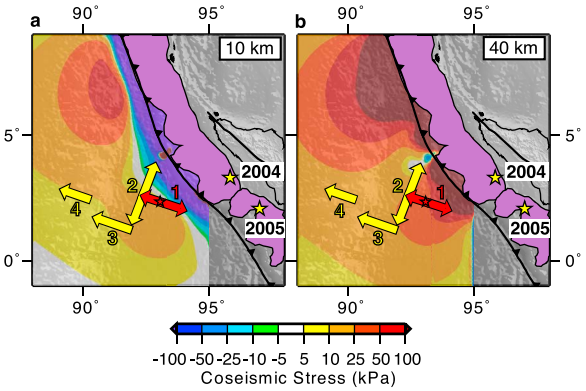

Figure 4. The effects of receiver depth. Coseismic stress changes resulting from the 2004 and 2005 earthquakes [*Chlieh et al.*, 2007; *Konca et al.*, 2007] resolved on the WNW-ESE (red) fault plane. Calculated at (a) 10 km depth, and (b) the deeper centroid depth of 40 km (see Figures S7 and S8 in the auxiliary material for other depths and stresses resolved on the NNE-SSW fault plane).

[8] The 2012 mainshock was able to grow to such a large magnitude because it was able to continue rupturing beyond the initial WNW-ESE fault plane, on multiple nearby faults in the weak, heavily fractured northern Wharton Basin. This complex rupture scenario is similar to the second largest Wharton Basin earthquake, a M_w 7.9 earthquake in June 2000, which started as left-lateral strike-slip motion on a N-S plane and ended as oblique motion on an E-W plane [*Abercrombie et al.*, 2003]. Several of the focal mechanisms for the first month of 2012 aftershocks show oblique-to-reverse motion, indicating that the M_w 8.6 earthquake may have included an oblique sub-event as well (see Figure S1 in the auxiliary material).[1] Although the orientation of maximum compression in the Wharton Basin would accommodate NE-SW oriented reverse faulting, reverse mechanisms are not common, likely because it is easier to reactivate the pre-existing faults and fracture zones.

4. Stress Changes Induced by the Megathrust Earthquakes

[9] We have calculated the stresses induced by the 2004 and 2005 megathrust earthquakes at the hypocenter of the M_w 8.6 earthquake in order to determine if the 2012 earthquakes were triggered events. We modeled the static, coseismic stress perturbations from the two nearby megathrust ruptures, using source models determined from the inversion of geodetic data [*Chlieh et al.*, 2007] and the joint inversion of seismic and geodetic data [*Konca et al.*, 2007]. The elastic coseismic deformation is calculated in a layered half-space using the EDGRN/EDCMP [*Wang et al.*, 2003] programs and a 1-D velocity structure representing the Sumatran forearc [*Collings et al.*, 2012]. The deformation calculations are used as input to model the Coulomb failure stress (CFS) changes on the orientation of the oceanic strike-slip earthquakes. ΔCFS is defined as the change in shear stress (positive in direction of fault slip) plus the effective coefficient of friction times the normal stress (unclamping is positive). We assume an effective coefficient of friction $\mu' = 0.4$, and determine the CFS changes on constant depth sections in the 2012 epicentral region. We resolve the stress changes on both of the nodal plane orientations associated with the 2012 mainshock.

[10] The 2004 earthquake contributed most of the stress changes at the 2012 hypocenter and further to the north spanning the zone of enhanced strike-slip activity (yellow focal mechanisms in Figures 3b and 3c). The combined coseismic stress perturbation from the 2004 and 2005 earthquakes was ~18 kPa at the hypocenter (Figure 3b), with similar values when resolving stress on either the WNW-ESW or NNE-SSW fault plane orientation (see Figure S2 in the auxiliary material).

[11] The positive stress lobe near the hypocenter is a robust feature. We compare our preferred coseismic stress model, based on the smoothed, higher resolution *Chlieh et al.* [2007] and *Konca et al.* [2007] megathrust source models that consider seismic and geodetic data sets, with the less discretized, geodetically based *Banerjee et al.* [2007] source models, and the 2012 hypocenter is still positively stressed on both fault orientations (see Figures S3 and S4 in the auxiliary material). The stress change at the 2012 hypocenter is most sensitive to the amount of slip, and the depth range of slip, on the southern portion of the 2004 rupture. More shallow slip on the southern portion of the 2004 rupture, as in the *Banerjee et al.* [2007] model, increases the positive stress change at the 2012 hypocenter and decreases the extent of the negative stress region near the trench (see Figures S3–S6 in the auxiliary material). *Lay et al.* [2011a, 2011b] have observed that Coulomb stress values in the region near the trench are very sensitive to the amount of shallow slip during the 2011 Tohoku megathrust earthquake. Unfortunately, the geodetic data are more limited for the 2004 Sumatran-Andaman earthquake, and it is not possible to uniquely resolve the amount of shallow slip on the southern segment. There were several strike-slip earthquakes in this sensitive region during the years following the 2004 earthquake that were either positively or negatively stressed depending on the coseismic source model. We also test a range of receiver fault depths from 10–40 km and find that the coseismic stress change increases with depth at the epicenter (Figure 4 and Figures S7 and S8 in the auxiliary material), especially in the region northeast of the hypocenter where *Yue et al.* [2012] model deep slip on both the WNW-ESE and NNE-SSW planes.

[12] We also calculate the time-dependent stress perturbations resulting from postseismic relaxation of the upper mantle following the megathrust events. Postseismic deformation resulting from viscoelastic relaxation of the asthenosphere is calculated on a layered, laterally-homogeneous, spherical earth using the method of *Pollitz* [1992]. We employ *Panet et al.*'s [2010] rheology model that fits the first ~3 years of horizontal far-field GPS time-series, and gravity variations recorded by the GRACE satellite, following the 2004 earthquake. This model includes a bi-viscous asthenosphere with an initial short-term viscosity of 4×10^{17} Pa s and a long-term viscosity of 8×10^{18} Pa s.

[13] By April 2012, the postseismic stress perturbation from the megathrust earthquakes was ~4 times larger than the induced coseismic stresses at the 2012 hypocenter, highlighting the importance of postseismic deformation for

[1] Auxiliary materials are available in the HTML. doi:10.1029/2012GL053954.

triggering earthquakes away from the coseismic rupture plane (see stress time series in Figures 2 and 3c). These additional stress perturbations can explain the continued strike-slip activity during the years following the 2004 earthquake (blue focal mechanisms in Figures 3b and 3c). This includes events NE of the 2012 hypocenter that experienced negative coseismic stress changes but positive postseismic stress perturbations, and the June 2010 and January 2012 M 7+ events.

[14] The postseismic deformation and associated stress perturbations are likely larger in the northern Wharton Basin than in the surrounding Indian Ocean due to the thinner and warmer lithosphere in this region [*Shapiro et al.*, 2008]. A locally thinner lithosphere in the vicinity of the 2012 earthquakes would allow larger stress transmissions from the closer, flowing asthenosphere, and the warmer mantle would increase the pace of viscous relaxation, inducing larger stress perturbations by the time of the 2012 earthquake. In addition, the January 2012 M_w 7.2 earthquake was located only ~25 km NE of the mainshock, also involving right-lateral slip on an E-W oriented fault (G. Hayes, Preliminary result of the Jan 10, 2012 Mw 7.2 off the west coast of northern Sumatra, Indonesia earthquake, 2012, available at http://earthquake.usgs.gov/earthquakes/eqinthenews/2012/usc0007ir5/finite_fault.php), and added a final push before the April events.

5. Discussion and Conclusions

[15] The high strain rates within the Wharton Basin enable strike-slip earthquakes over a wide portion of the plate interior, and the stresses imparted to the oceanic lithosphere by the 2004 earthquake induced a spike in the rate of these strike-slip earthquakes. Although megathrust ruptures in other tectonic settings would produce similar enhanced stresses along the orientation of the 2012 earthquake, in most cases there would not be enough accumulated strain in the oceanic plate, or pre-existing geologic structures, to enable such a large-magnitude triggered earthquake. For example, there were no triggered strike-slip earthquakes in the interior of the Pacific plate, east of the trench, during the 14 months following 2011 Tohoku earthquake (based on Global CMT catalog). The broad shear zone associated with the diffuse India-Australia plate boundary primed the northern Wharton Basin for strike-slip faulting and the megathrust earthquakes provided the triggering mechanism. The 2012 magnitude 8+ events were the latest in this collection of post-2004 strike-slip earthquakes and the additional stress imparted to the lithosphere from the postseismic deformation can explain the time delay between the 2004 and 2012 earthquakes.

[16] An independent study by *Delescluse et al.* [2012] also investigates the connection between the 2004 and 2005 megathrust earthquakes and the April 2012 oceanic earthquakes. They use different megathrust source models and simpler modeling approaches - homogeneous elastic half-space for the coseismic stress calculations and 2-D finite-element model with uniform imposed slip for the postseismic stress calculations - but come to similar conclusions. This emphasizes the robustness of the main results that the megathrust earthquakes enhanced seismicity in the northern Wharton Basin, both through static coseismic stress perturbations and through evolving postseismic stress transients.

[17] The 2012 mainshock was so large because it was able to rupture multiple weak spots within the oceanic lithosphere, including four separate fault planes. The annual moment rate for the entire Wharton Basin, that actively deforms down to 20°S, is $\sim 3.5 \times 10^{19}$ Nm/yr [*Delescluse and Chamot-Rooke*, 2007], and these two magnitude 8+ strike-slip earthquakes released ~270 years of accumulated seismic moment. The northern portion of Wharton Basin is the most rapidly straining region in the diffuse India-Australia boundary zone, accommodating roughly 1 cm/yr of N-S left-lateral shear over the past eight million years [*Delescluse and Chamot-Rooke*, 2007], so this region should have shorter earthquake repeat times of order of 500–1000 years, than the rest of the region. Over the past millennia, the megathrust earthquake periodicity for the southern end of the 2004 rupture has been roughly 400–600 years [*Meltzner et al.*, 2010], and therefore great oceanic strike-slip earthquakes in the northern Wharton Basin may coincide with the Sunda megathrust earthquakes every 1–2 cycles. This quasi-phase locking between the megathrust and strike-slip faulting in the northern Wharton Basin is speculative, but could be similar to the fault synchronization observed by *Scholz* [2010] in the Iceland seismic zone, Central Nevada seismic belt, and the Eastern California shear zone. Although these 2012 earthquakes did not cause much damage or casualties, they highlight the risk that very large earthquakes can occur away from major plate boundaries, and that unexpected events can be triggered well after great megathrust earthquakes.

[18] **Acknowledgments.** This work has been supported by NSF grant EAR-0738299 (to R.B.). We acknowledge comments by Rachel Abercrombie and an anonymous reviewer, and two anonymous reviewers of a previous version of this paper. The figures in this paper were produced using the GMT software. This is Berkeley Seismological Laboratory contribution 11-10.

[19] The Editor thanks two anonymous reviewers for their assistance in evaluating this paper.

References

Abercrombie, R., M. Antolik, and G. Ekström (2003), The June 2000 M_w 7.9 earthquakes south of Sumatra: Deformation in the India-Australia Plate, *J. Geophys. Res.*, *108*(B1), 2018, doi:10.1029/2001JB000674.

Amante, C., and B. W. Eakins (2009), ETOPO1 1 arc-minute global relief model: Procedures, data sources and analysis, *NOAA Tech. Memo. NESDIS NGDC-24*, 19 pp., NOAA, Silver Spring, Md.

Banerjee, P., F. Pollitz, B. Nagarajan, and R. Bürgmann (2007), Coseismic slip distributions of the 26 December 2004 Sumatra-Andaman and 28 March 2005 Nias earthquakes from GPS static offsets, *Bull. Seismol. Soc. Am.*, *97*, S86–S102, doi:10.1785/0120050609.

Cattin, R., N. Chamot-Rooke, M. Pubellier, A. Rabaute, M. Delescluse, C. Vigny, L. Fleitout, and P. Dubernet (2009), Stress change and effective friction coefficient along the Sumatra-Andaman-Sagaing fault system after the 26 December 2004 (M_w = 9.2) and the 28 March 2005 (M_w = 8.7) earthquakes, *Geochem. Geophys. Geosyst.*, *10*, Q03011, doi:10.1029/2008GC002167.

Chlieh, M., et al. (2007), Coseismic slip and afterslip of the great M_w 9.15 Sumatra-Andman earthquake of 2004, *Bull. Seismol. Soc. Am.*, *97*, S152–S173, doi:10.1785/0120050631.

Collings, R., D. Lange, A. Rietbrock, F. Tilmann, D. Natawidjaja, B. Suwargadi, M. Miller, and J. Saul (2012), Structure and seismogenic properties of the Mentawai segment of the Sumatra subduction zone revealed by local earthquake traveltime tomography, *J. Geophys. Res.*, *117*, B01312, doi:10.1029/2011JB008469.

Delescluse, M., and N. Chamot-Rooke (2007), Instantaneous deformation and kinematics of the India-Australia Plate, *Geophys. J. Int.*, *168*, 818–842, doi:10.1111/j.1365-246X.2006.03181.x.

Delescluse, M., et al. (2012), April 2012 intra-oceanic seismicity off Sumatra boosted by the Banda-Aceh megathrust, *Nature*, *490*, 240–244, doi:10.1038/nature11520.

Deplus, C. (2001), Indian ocean actively deforms, *Science*, *292*, 1850–1851, doi:10.1126/science.1061082.

Deplus, C., et al. (1998), Direct evidence of active deformation in the eastern Indian oceanic plate, *Geology*, *26*, 131–134, doi:10.1130/0091-7613(1998)026<0131:DEOADI>2.3.CO;2.

Hill, E. M., et al. (2012), The 2010 M_w 7.8 Mentawai earthquake: Very shallow source of a rare tsunami earthquake determined from tsunami field survey and near-field GPS data, *J. Geophys. Res.*, *117*, B06402, doi:10.1029/2012JB009159.

Konca, A. O., et al. (2007), Rupture kinematics of the 2005 M_w 8.6 Nias-Simeulue earthquake from the joint inversion of seismic and geodetic data, *Bull. Seismol. Soc. Am.*, *97*, S307–S322, doi:10.1785/0120050632.

Konca, A. O., et al. (2008), Partial rupture of a locked patch of the Sumatra megathrust during the 2007 earthquake sequence, *Nature*, *456*, 631–635, doi:10.1038/nature07572.

Lay, T., C. J. Ammon, H. Kanamori, L. Xue, and M. J. Kim (2011a), Possible large near-trench slip during the 2011 Mw 9.0 off the Pacific coast Tohoku earthquake, *Earth Planets Space*, *63*, 687–692, doi:10.5047/eps.2011.05.033.

Lay, T., C. J. Ammon, H. Kanamori, M. J. Kim, and L. Xue (2011b), Outer trench-slope faulting and the 2011 Mw 9.0 off the Pacific coast of Tohoku earthquake, *Earth Planets Space*, *63*, 713–718, doi:10.5047/eps.2011.05.006.

McCloskey, J., S. S. Nalbant, and S. Steacy (2005), Earthquake risk from co-seismic stress, *Nature*, *434*, 291, doi:10.1038/434291a.

McCloskey, J., et al. (2010), The September 2009 Padang earthquake, *Nat. Geosci.*, *3*, 70–71, doi:10.1038/ngeo753.

McGuire, J. J., and G. C. Beroza (2012), A rogue earthquake off Sumatra, *Science*, *336*, 1118–1119, doi:10.1126/science.1223983.

Meltzner, A. J., K. Sieh, H.-W. Chiang, C.-C. Shen, B. W. Suwargadi, D. H. Natawidjaja, B. E. Philibosian, R. W. Briggs, and J. Galetzka (2010), Coral evidence for earthquake recurrence and an A.D. 1390–1455 cluster at the south end of the 2004 Aceh–Andaman rupture, *J. Geophys. Res.*, *115*, B10402, doi:10.1029/2010JB007499.

Meng, L., et al. (2012), Earthquake in a maze: compressional rupture branching during the April 11 2012 M_w 8.6 Sumatra earthquake, *Science*, *337*, 724–726, doi:10.1126/science.1224030.

Nalbant, S. S., S. Steacy, K. Sieh, D. Natawidjaja, and J. McCloskey (2005), Earthquake risk on the Sunda trench, *Nature*, *435*, 756–757, doi:10.1038/nature435756a.

Panet, I., F. Pollitz, V. Mikhailov, M. Diament, P. Banerjee, and K. Grijalva (2010), Upper mantle rheology from GRACE and GPS postseismic deformation after the 2004 Sumatra-Andaman earthquake, *Geochem. Geophys. Geosyst.*, *11*, Q06008, doi:10.1029/2009GC002905.

Pollitz, F. F. (1992), Postseismic relaxation theory on the spherical earth, *Bull. Seismol. Soc. Am.*, *82*, 422–453.

Sager, W. W., C. F. Paul, K. S. Krishna, M. Pringle, A. E. Eisin, F. A. Frey, D. Gopala Rao, and O. Levchenko (2010), Large fault fabric of the Ninetyeast Ridge implies near-spreading ridge formation, *Geophys. Res. Lett.*, *37*, L17304, doi:10.1029/2010GL044347.

Satriano, C., E. Kiraly, P. Bernard, and J.-P. Vilotte (2012), The 2012 Mw 8.6 Sumatra earthquake: Evidence of westward sequential seismic ruptures associated to the reactivation of a N-S ocean fabric, *Geophys. Res. Lett.*, *39*, L15302, doi:10.1029/2012GL052387.

Scholz, C. H. (2010), Large earthquake triggering, clustering, and the synchronization of faults, *Bull. Seismol. Soc. Am.*, *100*, 901–909, doi:10.1785/0120090309.

Sevilgen, V., R. S. Stein, and F. F. Pollitz (2012), Stress imparted by the great 2004 Sumatra quake shut down transforms and activated rifts up to 400 km away in the Andaman Sea, *Proc. Natl. Acad. Sci. U. S. A.*, doi:10.1073/pnas.1208799109.

Shapiro, N. M., M. H. Ritzwoller, and E. R. Engdahl (2008), Structural context of the great Sumatra-Andaman Islands earthquake, *Geophys. Res. Lett.*, *35*, L05301, doi:10.1029/2008GL033381.

Shearer, P., and R. Bürgmann (2010), Lessons learned from the 2004 Sumatra-Andaman megathrust rupture, *Annu. Rev. Earth Planet. Sci.*, *38*, 103–131, doi:10.1146/annurev-earth-040809-152537.

Singh, C., et al. (2011), Extremely thin crust in the Indian Ocean possibly resulting from plume-ridge interaction, *Geophys. J. Int.*, *184*, 29–42, doi:10.1111/j.1365-246X.2010.04823.x.

Wang, R., F. L. Martin, and F. Roth (2003), Computation of deformation induced by earthquakes in a multi-layered elastic crust—FORTRAN programs EDGRN/EDCMP, *Comput. Geosci.*, *29*, 195–207, doi:10.1016/S0098-3004(02)00111-5.

Wiseman, K., and R. Bürgmann (2011), Stress and seismicity changes on the Sunda megathrust preceding the 2007 M_w 8.4 earthquake, *Bull. Seismol. Soc. Am.*, *101*, 313–326, doi:10.1785/0120100063.

Wiseman, K., P. Banerjee, K. Sieh, R. Bürgmann, and D. H. Natawidjaja (2011), Another potential source of destructive earthquakes and tsunami offshore of Sumatra, *Geophys. Res. Lett.*, *38*, L10311, doi:10.1029/2011GL047226.

Wiseman, K., P. Banerjee, R. Bürgmann, K. Sieh, D. Dreger, and I. Hermawan (2012), Source model of the 2009 M_w 7.6 Padang intraslab earthquake and its effect on the Sunda megathrust, *Geophys. J. Int.*, *190*, 1710–1722, doi:10.1111/j.1365-246X.2012.05600.x.

Yue, H., T. Lay, and K. D. Koper (2012), En echelon and orthogonal fault ruptures of the 11 April 2012 great intraplate earthquakes, *Nature*, *490*, 245–249, doi:10.1038/nature11492.